

Heavy top renormalon contribution to fermion propagatorsD. Bettinelli^{1,*} and J. J. van der Bij^{2,†}¹*INFN, Sezione di Milano via Celoria 16, I-20133 Milano, Italy*²*Physikalisches Institut, Albert-Ludwigs-Universität Freiburg, Hermann-Herder-Strasse 3, D-79104 Freiburg im Breisgau, Germany*

(Received 11 June 2012; published 15 August 2012)

We study resummed perturbative contributions due to a heavy top quark. These renormalon contributions are evaluated for fermion propagators. Results for the top-quark width are given. Estimates of nonperturbative uncertainties are made on the ρ parameter using different schemes of dealing with the Landau pole. For the physical top-quark mass the effects are negligible.

DOI: [10.1103/PhysRevD.86.045018](https://doi.org/10.1103/PhysRevD.86.045018)

PACS numbers: 11.15.Pg, 11.15.Tk, 14.65.Ha

I. INTRODUCTION

In the electroweak sector of the standard model (SM) every particle acquires its mass through an interaction with a scalar potential in a nontrivial vacuum. As a consequence, all the masses are proportional to a common scale, namely $G_F^{-1/2}$, which is fixed by low-energy measurements such as the μ -decay rate. In this situation the decoupling theorem [1] does not hold, and thus there exist low-energy observables in which the quantum effects induced by virtual heavy particles do not vanish when the mass of these particles goes to infinity.

Most prominent among the nondecoupling effects is the ρ parameter [2], which provides a measure of the relative strength of neutral and charged current interactions in four fermion processes at zero momentum transfer. At tree level $\rho = 1$ due to a global accidental $SU(2)$ symmetry, the so-called custodial symmetry. ρ can receive radiative corrections only by those sectors of the SM that break explicitly the custodial symmetry, namely, the hypercharge and the Yukawa couplings that give different masses to the components of fermion doublets. In the latter case the contribution to the ρ parameter is proportional to the mass splitting; therefore the leading contribution comes from the top-bottom doublet.

At one loop the ρ parameter has a quadratic dependence on the top-quark mass, $\Delta\rho^{(1)} \approx G_F m_t^2$, and a logarithmic dependence on the Higgs mass, $\Delta\rho^{(1)} \approx g'^2 \log(\frac{m_H}{M_W})$. Two-loop corrections at the leading order, i.e. $\Delta\rho^{(2)} \approx G_F^2 m_t^4$, and at the next-to-leading order, i.e. $\Delta\rho^{(2)} \approx G_F^2 m_t^2 M_Z^2$, in the top-quark mass were computed in the limits $m_H \rightarrow 0$ and $m_H \gg m_t$ in Refs. [3,4] and for arbitrary Higgs mass in Ref. [5]. It turned out that due to accidental cancellations, the subleading corrections at two loops are larger than the leading ones [6]. At three loops the computation of the leading top-quark corrections, $\Delta\rho^{(3)} \approx G_F^3 m_t^6$, in the massless Higgs limit, was carried out in Ref. [7]. The

complete dependence on the Higgs mass at three loops was obtained in Ref. [8]. Numerically it was found that this contribution to $\Delta\rho$ is quite large and provides a sizable correction ($\approx 36\%$) to the leading electroweak correction at two loops. However, the size of the three-loop correction is only about 2% of the much larger two-loop subleading electroweak correction. Moreover, the perturbative series of the leading top-quark contributions to the ρ parameter has alternating signs up to three loops.

This raises the issue of the convergence of the perturbative expansion (it might be that this series is divergent, but Borel summable) and calls for a better understanding of higher order radiative corrections. It would be highly desirable to have a simplified framework in which the leading top-quark contributions to the ρ parameter can be computed to all orders in perturbation theory and eventually summed up. The actual calculation of the leading radiative corrections in the top-quark mass is greatly simplified by the observation that to obtain them it is enough to consider the Lagrangian of the SM in the limit of vanishing gauge coupling constants $g, g' \rightarrow 0$ [4]. This gaugeless limit provides an efficient way of reducing the number of Feynman diagrams to be computed, and it has been used in the two- and three-loop computations mentioned above.

In some recent papers [9,10] the effects of a finite top width were resummed by using a $SU(N_F) \times U(1)$ electroweak model in the large N_F limit [11,12]. In this paper we will use another resummation procedure. In the model we are going to study, the symmetry group is the one of the SM, namely $SU(2) \times U(1)$, but instead of having three generations of quarks and leptons we consider a large number of copies (N_G) of the third family of quarks. In order to avoid the presence of chiral anomalies we have to take into account an equal number of copies of the third family of leptons; however, this will play no role in the further calculations. All of the extra quark doublets contain a massive particle, the top-quark with mass m_t , and a massless particle, the bottom quark, while both components of the extra lepton doublets are taken to be massless. Notice that this is not meant to be phenomenologically relevant. Indeed, from LEP ($Z \rightarrow \bar{\nu}\nu$) we know that there

*daniele.bettinelli@mi.infn.it

†jochum@physik.uni-freiburg.de

are only three generations of light neutrinos. We take the approximation that the Cabibbo-Kobayashi-Maskawa matrix is diagonal. The large N_G limit is performed by keeping $y_i^2 N_G$ fixed, where y_i is the top-Yukawa coupling. In this limit only the graphs with a maximal number of fermion loops contribute. This sort of sum is known as a renormalon chain [13].

As we are working in the limit of a heavy top quark the effects of the gauge couplings can be ignored, and we have a resummed propagator in the Higgs and the Goldstone-boson sector only. The resulting Dyson propagators contain, in addition to the physical pole, a tachyon pole in the Euclidean region, $p^2 = -\Lambda_T^2$, which spoils causality and makes the Wick-rotated Feynman integrals ill defined.

If one wants to use the resummed propagators in further loop insertions, one has to find a way to treat this tachyon pole. In this connection the introduction of an UV cutoff at $\Lambda < \Lambda_T$ has been proposed in Ref. [14]. However, this procedure breaks gauge invariance. We have adopted another strategy that was used successfully in Ref. [15]. Assuming that the occurrence of the tachyon pole is not due to the inconsistency of the theory under consideration, but of the intermediary expansion technique used, it is reasonable to simply subtract the tachyon-pole minimally from the propagator, thereby restoring causality. This is actually a rather old idea [16] that has been adapted in a slightly modified form in QCD under the name of analytic perturbation theory [17].

One should be careful in doing this because the tachyon pole contributes to the Källén-Lehmann spectral function. Further corrections might be needed in order to preserve fundamental aspects of the theory. In analytic perturbation theory, for instance, the tachyon subtraction was done at the level of the effective charge. On the propagator level this corresponds to subtracting the tachyon pole and adding it back with the same strength at $p^2 = 0$. This is necessary in order to preserve asymptotic freedom. Technically one deals with a subtracted dispersion relation. In another context [18], resummation inside the Higgs propagator, the normalization of the spectral density was essential, and one had to multiply the propagator with a constant nonperturbative factor.

Unfortunately the addition of nonperturbative factors is not unique, as was already mentioned in the earliest paper [16]. Nonetheless, it is important to get some idea on the size of possible nonperturbative effects. A theory that is only defined in the perturbative approximation is, of course, not satisfactory. This is also true for the standard model. Ultimately, one will try to put the theory on the lattice in order to go beyond perturbation theory. Since the electroweak sector of the SM is not asymptotically free, presumably cutoff effects stay present in the lattice predictions. The situation is complicated due to the presence of fermion doubles on the lattice, which one cannot remove as easily as in lattice QCD by moving their mass to infinity,

since they get their mass via the Higgs mechanism and therefore become strongly coupled in this limit. In order to compare with the continuum, the use of resummed propagators is at the moment the only alternative, whereby the uncertainty due to the nonperturbative effects should correspond to the uncertainty in predictions due to the cutoff effects on the lattice. It is to be remarked, however, that even with $m_t = 172$ GeV perturbation theory is quite satisfactory. As the Higgs boson is also presumably light, from the practical point of view perturbation theory should be good enough for the SM.

In this paper we calculate the contribution of the resummed propagators to the top- and bottom-quark propagators. These contributions can then be used as input for further calculations but are of interest by themselves. The outline of the paper is as follows. In Sec. II we discuss the resummed Higgs and would-be Goldstone-boson propagators. In Sec. III we discuss possible nonperturbative contributions to the ρ parameter due to alternative treatments of the tachyon. In Sec. IV we present results on the top propagator, due to the insertions of resummed propagators in a loop. Section V deals with the bottom propagator. In Sec. VI we give conclusions and outlook. The appendices contain the relevant part of the Lagrangian and the formulas for the one-loop integrals.

II. ONE-LOOP SELF-ENERGIES AT THE LEADING ORDER IN THE FLAVOR EXPANSION

In this section we shall give the expressions of the on-shell renormalized one-loop self-energies of the scalar particles (Higgs and would-be Goldstone bosons) at the leading order in the flavor expansion. Moreover, the subtraction of tachyonic poles from the Dyson resummed propagators will be presented. We perform the calculation in the Landau gauge, in order to have massless unphysical scalars, and we keep only two mass scales, namely, the top-quark, m_t , and the Higgs boson mass, m_H .

A. Neutral would-be Goldstone boson

In this subsection we discuss the self-energy of the neutral would-be Goldstone boson, χ , at the leading order in the large N_G expansion. The two graphs contributing to $\Sigma_\chi(p^2)$, which are enhanced by a factor N_G , are depicted in Fig. 1. The sum of these graphs is given by (for the notation see Appendix B)

$$\Sigma_\chi(p^2) = 2i\sqrt{2}N_c N_G G_F m_t^2 p^2 B_0[p^2, m_t, m_t], \quad (1)$$

where N_c is the number of colors, while N_G is the number of copies of the third generation. The on-shell renormalized χ self-energy, reads

$$\hat{\Sigma}_\chi(p^2) = \Sigma_\chi(p^2) - \delta m_\chi^2 + \delta Z_\chi p^2, \quad (2)$$

where the mass counterterm, δm_χ^2 , and the wave function renormalization constant, δZ_χ , are given by

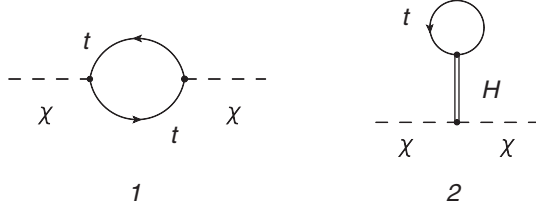


FIG. 1. SM enhanced contribution to the one-loop χ self-energy.

$$\begin{aligned} \delta m_\chi^2 &= \Sigma_\chi(p^2 = 0) = 0, \\ \delta Z_\chi &= -\Sigma'_\chi(p^2 = 0) = -\alpha_t \left[\frac{2}{D-4} + \log\left(\frac{m_t^2}{\Lambda_B^2}\right) + 2 \right]. \end{aligned} \quad (3)$$

In the above equation we have introduced a shorthand notation $\alpha_t = \frac{\sqrt{2}}{8\pi^2} N_c N_G G_F m_t^2$. We remind the reader that in the SM one has $N_c = 3$, $N_G = 1$, and $\alpha_t = 0.0187$.

The renormalized self-energy below the production threshold, $p^2 < 4m_t^2$, reads

$$\begin{aligned} \hat{\Sigma}_\chi(p^2) &= \alpha_t p^2 \left[2\sqrt{-\Delta_\chi} \arctan\left(\frac{1}{\sqrt{-\Delta_\chi}}\right) - 2 \right], \\ \Delta_\chi &= 1 - \frac{4m_t^2}{p^2}. \end{aligned} \quad (4)$$

The expression for the on-shell renormalized χ self-energy above the production threshold is given by

$$\begin{aligned} \hat{\Sigma}_\chi(p^2) &= \alpha_t p^2 \left\{ \frac{\sqrt{\Delta_\chi}}{2} \log \left[\frac{(1 + \sqrt{\Delta_\chi})p^2 - 2m_t^2}{(1 - \sqrt{\Delta_\chi})p^2 - 2m_t^2} \right] \right. \\ &\quad \left. - 2 - i\pi\sqrt{\Delta_\chi} \right\}. \end{aligned} \quad (5)$$

The behavior of the renormalized self-energy for large momentum is

$$\hat{\Sigma}_\chi(p^2) = \alpha_t p^2 \left[\log\left(-\frac{p^2}{m_t^2} - i\epsilon\right) - 2 \right], \quad \text{for } p^2 \gg m_t^2. \quad (6)$$

The Dyson resummed propagator of the neutral would-be Goldstone boson χ at the leading order in the large N_G limit is given by

$$\hat{D}_\chi(p^2) = \frac{i}{p^2 - \hat{\Sigma}_\chi(p^2) + i\epsilon}. \quad (7)$$

Besides the real pole at $p^2 = 0$ corresponding to the neutral would-be Goldstone boson, the exact χ propagator in Eq. (7) contains a tachyon pole. Its Euclidean position, $p^2 = -\Lambda_{T,\chi}^2$, can be obtained by solving numerically the following equation:

$$\begin{aligned} \sqrt{1 + \frac{4}{\lambda_{T,\chi}^2}} \log \left[\frac{\lambda_{T,\chi}^2 + 2 + \sqrt{\lambda_{T,\chi}^4 + 4\lambda_{T,\chi}^2}}{\lambda_{T,\chi}^2 + 2 - \sqrt{\lambda_{T,\chi}^4 + 4\lambda_{T,\chi}^2}} \right] &= \frac{2}{\alpha_t} + 4, \\ \lambda_{T,\chi}^2 &= \frac{\Lambda_{T,\chi}^2}{m_t^2}. \end{aligned} \quad (8)$$

A crude estimation of the position of the tachyonic pole can be given by using the approximate expression in Eq. (6) instead of the full one

$$\Lambda_{T,\chi}^2 \simeq m_t^2 \exp\left(\frac{1}{\alpha_t} + 2\right). \quad (9)$$

In Fig. 2 we show a comparison between the exact position of the tachyon (divided by the top-quark mass) and the approximated expression in the above equation. The latter nicely reproduces the exact result for $\alpha_t < 1$, while for bigger values of the coupling constant it starts overestimating it.

The residuum at the tachyon pole, κ_χ , can be computed exactly in terms of $\lambda_{T,\chi}^2$,

$$\frac{1}{\kappa_\chi} = -\alpha_t + \frac{4\alpha_t + 2}{\lambda_{T,\chi}^2 + 4}. \quad (10)$$

The opposite of the residuum, $-\kappa_\chi$, is plotted against α_t together with its approximation, $-\kappa_\chi = \frac{1}{\alpha_t}$, in Fig. 3.

The spectral representation of the χ propagator (7) is given by

$$\hat{D}_\chi(p^2) = \int_{-\infty}^{+\infty} ds \frac{i\rho^\chi(s)}{p^2 - s + i\epsilon}, \quad (11)$$

where $\rho^\chi(s) = \rho_T^\chi(s) + \delta(s) + \rho_+^\chi(s)\theta(s - 4m_t^2)$.

Notice that due to the tachyonic contribution to the spectral function,

$$\rho_T^\chi(s) = \kappa_\chi \delta(s + \Lambda_{T,\chi}^2), \quad (12)$$

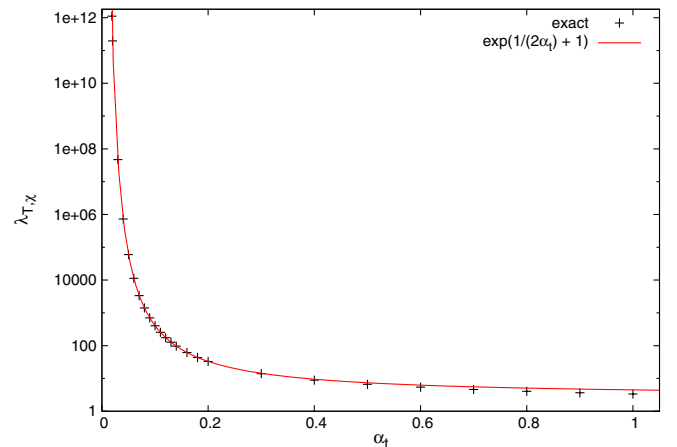


FIG. 2 (color online). Comparison between the exact result for $\lambda_{T,\chi}$ and its approximation.

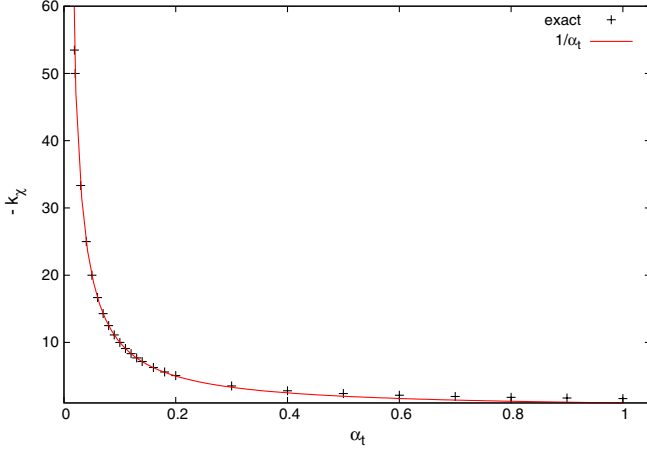


FIG. 3 (color online). Comparison between the exact result for $-\kappa_\chi$ and its approximation.

the exact χ propagator (7) does not satisfy the usual Källén–Lehmann spectral representation. The other contribution to the spectral function, which comes from the positive part of the spectrum, is given by

$$\rho_+^\chi(s) = \frac{\alpha_t}{s} \frac{\sqrt{\Delta_\chi}}{\left\{1 - \alpha_t \left[\frac{\sqrt{\Delta_\chi}}{2} \log \left[\frac{(1 + \sqrt{\Delta_\chi})s - 2m_t^2}{(1 - \sqrt{\Delta_\chi})s - 2m_t^2} \right] - 2 \right\]^2 + \pi^2 \alpha_t^2 \Delta_\chi} \right. \quad (13)$$

The integral over the spectrum of ρ_+^χ is convergent, since in the high-energy limit one has

$$\rho_+^\chi(s) \simeq \frac{\alpha_t}{s} \frac{1}{\left[1 - \alpha_t \log\left(\frac{s}{m_t^2}\right) + 2\alpha_t\right]^2 + \pi^2 \alpha_t^2}. \quad (14)$$

Notice that this is not the case in perturbation theory. Indeed, if one expands Eq. (13) in powers of α_t , the resulting spectral function at the leading perturbative order,

$$\rho_+^\chi(s) = \frac{\alpha_t}{s} \sqrt{1 - \frac{4m_t^2}{s}} + O(\alpha_t^2), \quad (15)$$

is clearly not integrable over the positive part of the spectrum. Thus, the resummation provides a cutoff to the theory.

By using the residue theorem, one can prove that the integral over the whole spectrum of the spectral function, ρ^χ , vanishes,

$$\int_{-\infty}^{+\infty} ds \rho^\chi(s) = \kappa_\chi + 1 + \int_{4m_t^2}^{+\infty} ds \rho_+^\chi(s) = 0. \quad (16)$$

The above result can also be checked with a careful numerical integration.

Clearly, the removal of the tachyonic pole is necessary in order to find an expression for the resummed χ propagator

that respects causality and satisfies the Källén–Lehmann representation. On the other hand, the contribution of the tachyon pole is crucial in order to ensure the normalization of the spectral function in Eq. (16). We propose to minimally subtract the tachyonic pole

$$\hat{D}_\chi^{\text{MS}}(p^2) = \frac{i}{p^2 - \hat{\Sigma}_\chi(p^2) + i\epsilon} - \frac{i\kappa_\chi}{p^2 + \Lambda_{\chi,T}^2}. \quad (17)$$

Furthermore, one can impose the condition that the integral over the physical, subtracted, spectral density be equal to one. This amounts to rescaling the subtracted propagator by a factor $-\frac{1}{\kappa_\chi}$. We call this prescription the Akhoury scheme in the following [18].

Another possibility is to perform a nonminimal subtraction of the tachyon (for a similar strategy in the context of QCD see Refs. [19]). One can, for instance, subtract the tachyonic pole and add its residuum to the pion pole at $p^2 = 0$. This prescription will be called beyond-the-minimal-subtraction (bMS) scheme,

$$\hat{D}_\chi^{\text{bMS}}(p^2) = \frac{i}{p^2 - \hat{\Sigma}_\chi(p^2) + i\epsilon} + \frac{i\kappa_\chi \Lambda_{\chi,T}^2}{p^2(p^2 + \Lambda_{\chi,T}^2)}. \quad (18)$$

This solution has the property of removing the tachyon without modifying the normalization of the spectral function. Indeed, one finds

$$\hat{D}_\chi^{\text{bMS}}(p^2) = \int_0^{+\infty} ds \frac{i\rho_{\text{bMS}}^\chi(s)}{p^2 - s + i\epsilon}, \quad (19)$$

where $\rho_{\text{bMS}}^\chi(s) = (1 + \kappa_\chi)\delta(s) + \rho_+^\chi(s)\theta(s - 4m_t^2)$.

We remark that there are other nonminimal ways of removing the tachyon. Another choice could be to impose the validity of the tree-level relation, i.e. integral of the spectral function equal to one. In the latter case the subtraction term is such that the resulting spectral function is given by

$$\rho^\chi(s) = (2 + \kappa_\chi)\delta(s) + \rho_+^\chi(s)\theta(s - 4m_t^2). \quad (20)$$

However, due to the lack of a subsidiary principle, like asymptotic freedom in QCD, we adopt, for the sake of simplicity, the minimal subtraction prescription in our computation of renormalon contribution to the top- and bottom-quark propagators.

B. Charged would-be Goldstone boson

In this subsection we shall discuss the self-energy of the charged would-be Goldstone boson, ϕ , at the leading order in the large N_G expansion. The two graphs contributing to $\Sigma_\phi(p^2)$, which are enhanced by a factor N_G , are depicted in Fig. 4. The sum of these graphs is given by (for the notation see Appendix B)

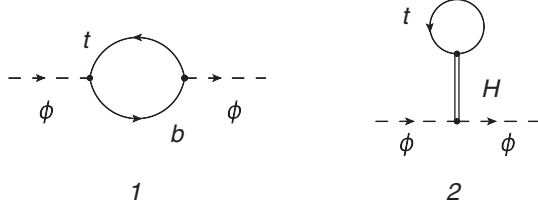


FIG. 4. SM enhanced contribution to the one-loop ϕ self-energy.

$$\begin{aligned} \Sigma_\phi(p^2) &= 2i\sqrt{2}N_c N_G G_F m_t^2 [(p^2 - m_t^2) \\ &\quad \times B_0[p^2, m_t, 0] + A_0[m_t]]. \end{aligned} \quad (21)$$

The on-shell renormalized ϕ self-energy reads

$$\hat{\Sigma}_\phi(p^2) = \Sigma_\phi(p^2) - \delta m_\phi^2 + \delta Z_\phi p^2, \quad (22)$$

where the mass counterterm, δm_ϕ^2 , and the wave function renormalization constant, δZ_ϕ , are given by

$$\delta m_\phi^2 = \Sigma_\phi(p^2 = 0) = 0, \quad (23)$$

$$\delta Z_\phi = -\Sigma'_\phi(p^2 = 0) = -\alpha_t \left[\frac{2}{D-4} + \log\left(\frac{m_t^2}{\Lambda_B^2}\right) + \frac{3}{2} \right].$$

The renormalized self-energy below the production threshold, $p^2 < m_t^2$, reads

$$\begin{aligned} \hat{\Sigma}_\phi(p^2) &= \alpha_t p^2 \left[\Delta_\phi^2 \log\left(\frac{-\Delta_\phi}{1 - \Delta_\phi}\right) - \Delta_\phi - \frac{1}{2} \right], \\ \Delta_\phi &= 1 - \frac{m_t^2}{p^2}. \end{aligned} \quad (24)$$

The expression for the on-shell renormalized ϕ self-energy above the production threshold is given by

$$\hat{\Sigma}_\phi(p^2) = \alpha_t p^2 \left[\Delta_\phi^2 \log\left(\frac{\Delta_\phi}{1 - \Delta_\phi}\right) - \Delta_\phi - \frac{1}{2} - i\pi \Delta_\phi^2 \right]. \quad (25)$$

The behavior of the renormalized self-energy for large momentum is

$$\begin{aligned} \hat{\Sigma}_\phi(p^2) &= \alpha_t p^2 \left[\log\left(-\frac{p^2}{m_t^2} - i\epsilon\right) - \frac{3}{2} \right], \\ &\quad \text{for } p^2 \gg m_t^2. \end{aligned} \quad (26)$$

The Dyson resummed propagator of the charged would-be Goldstone boson ϕ at the leading order in the large N_G limit is given by

$$\hat{D}_\phi(p^2) = \frac{i}{p^2 - \hat{\Sigma}_\phi(p^2) + i\epsilon}. \quad (27)$$

Besides the real pole at $p^2 = 0$ corresponding to the charged would-be Goldstone boson, the exact ϕ propagator in Eq. (27) contains a tachyon pole. Its Euclidean position, $p^2 = -\Lambda_{T,\phi}^2$, can be obtained by solving numerically the following equation:

$$\begin{aligned} \left(1 + \frac{1}{\lambda_{T,\phi}^2}\right)^2 \left[\log(\lambda_{T,\phi}^2 + 1) - \frac{\lambda_{T,\phi}^2}{\lambda_{T,\phi}^2 + 1} \right] &= \frac{1}{\alpha_t} + \frac{1}{2}, \\ \lambda_{T,\phi}^2 &= \frac{\Lambda_{T,\phi}^2}{m_t^2}. \end{aligned} \quad (28)$$

A crude estimation of the position of the tachyonic pole can be given by using the approximate expression in Eq. (26) instead of the full one

$$\Lambda_{T,\phi}^2 \simeq m_t^2 \exp\left(\frac{1}{\alpha_t} + \frac{3}{2}\right). \quad (29)$$

In Fig. 5 we show a comparison between the exact position of the tachyon (divided by the top-quark mass) and the approximated expression in the above equation. The latter nicely reproduces the exact result for $\alpha_t < 1$, while for bigger values of the coupling constant it starts overestimating it.

The residuum at the tachyon pole, κ_ϕ , can be computed exactly in terms of $\lambda_{T,\phi}^2$

$$\frac{1}{\kappa_\phi} = -\alpha_t + \frac{\alpha_t + 2}{\lambda_{T,\phi}^2 + 1}. \quad (30)$$

The opposite of the residuum, $-\kappa_\phi$, is plotted against α_t together with its approximation, $-\kappa_\phi = \frac{1}{\alpha_t}$ in Fig. 6.

The spectral representation of the ϕ propagator (27) is given by

$$\hat{D}_\phi(p^2) = \int_{-\infty}^{+\infty} ds \frac{i\rho^\phi(s)}{p^2 - s + i\epsilon}, \quad (31)$$

$$\text{where } \rho^\phi(s) = \rho_T^\phi(s) + \delta(s) + \rho_+^\phi(s)\theta(s - m_t^2).$$

Notice that due to the tachyonic contribution to the spectral function,

$$\rho_T^\phi(s) = \kappa_\phi \delta(s + \Lambda_{T,\phi}^2), \quad (32)$$

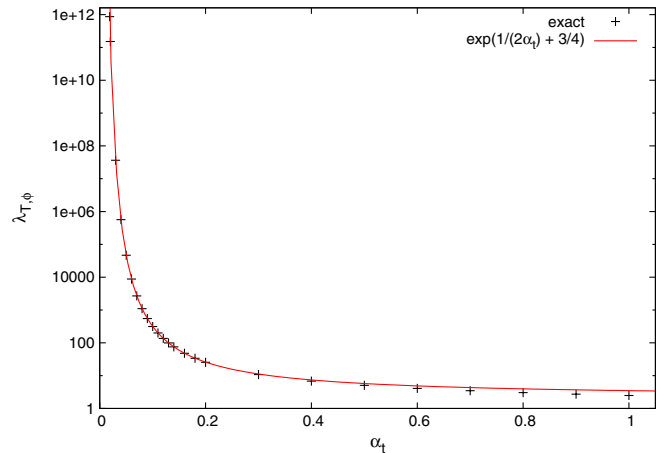


FIG. 5 (color online). Comparison between the exact result for $\lambda_{T,\phi}$ and its approximation.

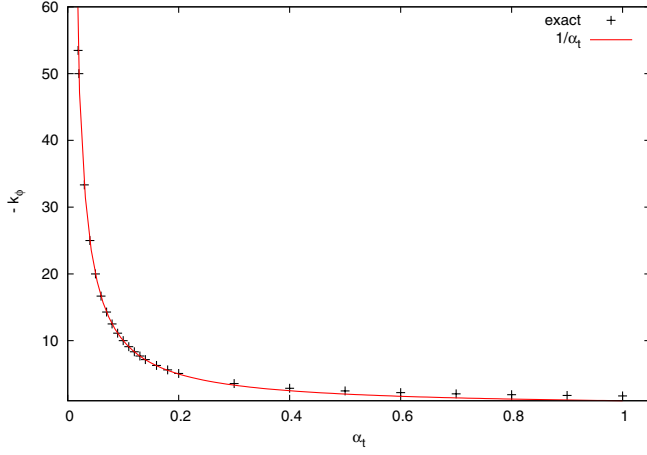


FIG. 6 (color online). Comparison between the exact result for $-\kappa_\phi$ and its approximation.

the exact ϕ propagator (27) does not satisfy the usual Källén–Lehmann spectral representation. The other contribution to the spectral function, which comes from the positive part of the spectrum, is given by

$$\rho_+^\phi(s) = \frac{\alpha_t}{s} \frac{\Delta_\phi^2}{\left\{1 - \alpha_t \left[\Delta_\phi^2 \log\left(\frac{\Delta_\phi}{1 - \Delta_\phi}\right) - \Delta_\phi - \frac{1}{2} \right] \right\}^2 + \pi^2 \alpha_t^2 \Delta_\phi^4}. \quad (33)$$

The integral over the spectrum of ρ_+^ϕ is convergent, since in the high-energy limit one has

$$\rho_+^\phi(s) \simeq \frac{\alpha_t}{s} \frac{1}{\left[1 - \alpha_t \log\left(\frac{s}{m_t^2}\right) + \frac{3}{2} \alpha_t\right]^2 + \pi^2 \alpha_t^2}. \quad (34)$$

Notice that, again, this is not the case in perturbation theory. By expanding the spectral function in Eq. (33) in powers of α_t , one gets a function,

$$\rho_+^\phi(s) = \frac{\alpha_t}{s} \left(1 - \frac{m_t^2}{s}\right)^2 + O(\alpha_t^2), \quad (35)$$

which is not integrable over the positive part of the spectrum.

By using the residue theorem, one can prove that the integral over the whole spectrum of ρ^ϕ vanishes

$$\int_{-\infty}^{+\infty} ds \rho^\phi(s) = \kappa_\phi + 1 + \int_{m_t^2}^{+\infty} ds \rho_+^\phi(s) = 0. \quad (36)$$

The above result has been confirmed by a careful numerical integration.

As in the neutral case we minimally subtract the tachyonic pole

$$\hat{D}_\phi^{\text{MS}}(p^2) = \frac{i}{p^2 - \hat{\Sigma}_\phi(p^2) + i\epsilon} - \frac{i\kappa_\phi}{p^2 + \Lambda_{\phi,T}^2}. \quad (37)$$

Normalizing the spectral density amounts to rescaling the subtracted propagator by a factor $-\frac{1}{\kappa_\phi}$.

In the case of the bMS scheme the tachyon-subtracted propagator is given by

$$\hat{D}_\phi^{\text{bMS}}(p^2) = \frac{i}{p^2 - \hat{\Sigma}_\phi(p^2) + i\epsilon} + \frac{i\kappa_\phi \Lambda_{\phi,T}^2}{p^2(p^2 + \Lambda_{\phi,T}^2)}. \quad (38)$$

Hereby one removes the tachyon, but keeps the spectral density normalized. One finds

$$\hat{D}_\phi^{\text{bMS}}(p^2) = \int_0^{+\infty} ds \frac{i\rho_{\text{bMS}}^\phi(s)}{p^2 - s + i\epsilon}, \quad (39)$$

where $\rho_{\text{bMS}}^\phi(s) = (1 + \kappa_\phi)\delta(s) + \rho_+^\phi(s)\theta(s - m_t^2)$.

C. Neutral Higgs boson

In this subsection we shall discuss the self-energy of the neutral Higgs boson at the leading order in the large N_G expansion. We consider a finite, but not completely arbitrary Higgs mass, namely $m_H < 2m_t$. In this way the Higgs boson cannot decay in $t\bar{t}$, and thus, it is stable at the leading order in the large N_G limit. The two graphs contributing to $\hat{\Sigma}_H(p^2)$, which are enhanced by a factor N_G , are depicted in Fig. 7. The sum of these graphs is given by (for the notation see Appendix B)

$$\begin{aligned} \hat{\Sigma}_H(p^2) &= 2i\sqrt{2}N_c N_G G_F m_t^2 [(p^2 - 4m_t^2) \\ &\quad \times B_0[p^2, m_t, m_t] + 4A_0[m_t]]. \end{aligned} \quad (40)$$

The on-shell renormalized Higgs self-energy reads

$$\hat{\hat{\Sigma}}_H(p^2) = \hat{\Sigma}_H(p^2) - \delta m_H^2 + \delta Z_H(p^2 - m_H^2), \quad (41)$$

where the mass counterterm, δm_H^2 , and the wave function renormalization constant, δZ_H , are given by

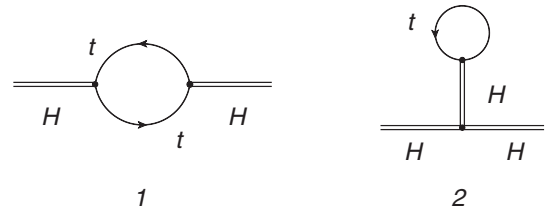


FIG. 7. SM enhanced contribution to the one-loop Higgs self-energy.

$$\begin{aligned}
\delta m_H^2 &= \Sigma_H(p^2 = m_H^2) \\
&= \alpha_t \left\{ m_H^2 \left[\frac{2}{D-4} + \log\left(\frac{m_t^2}{\Lambda_B^2}\right) + 2\sqrt{-\Delta_H} \arctan\left(\frac{1}{\sqrt{-\Delta_H}}\right) \right] + 4m_t^2 \left[1 - 2\sqrt{-\Delta_H} \arctan\left(\frac{1}{\sqrt{-\Delta_H}}\right) \right] \right\}, \\
\Delta_H &= 1 - \frac{4m_t^2}{m_H^2}, \\
\delta Z_H &= -\Sigma'_H(p^2 = m_H^2) = -\alpha_t \left[\frac{2}{D-4} + \log\left(\frac{m_t^2}{\Lambda_B^2}\right) + \Delta_H + 2\left(1 + \frac{2m_t^2}{m_H^2}\right) \sqrt{-\Delta_H} \arctan\left(\frac{1}{\sqrt{-\Delta_H}}\right) \right].
\end{aligned} \tag{42}$$

In the limit of vanishing Higgs mass, $m_H = 0$, one finds

$$\begin{aligned}
\delta m_H^2 &= -4\alpha_t m_t^2, \\
\delta Z_H &= -\alpha_t \left[\frac{2}{D-4} + \log\left(\frac{m_t^2}{\Lambda_B^2}\right) + \frac{8}{3} \right].
\end{aligned} \tag{43}$$

It is interesting to notice that there is a finite Higgs mass renormalization even if one neglects m_H . This effect comes from the vacuum expectation value of the Higgs field.

The renormalized Higgs self-energy below the production threshold, i.e. for $p^2 < 4m_t^2$, reads

$$\begin{aligned}
\hat{\Sigma}_H(p^2) &= \alpha_t p^2 \left\{ 2\Delta_\chi \left[\sqrt{-\Delta_\chi} \arctan\left(\frac{1}{\sqrt{-\Delta_\chi}}\right) - \sqrt{-\Delta_H} \arctan\left(\frac{1}{\sqrt{-\Delta_H}}\right) \right] \right. \\
&\quad \left. - \left(1 - \frac{m_H^2}{p^2}\right) \left[\Delta_H + \frac{4m_t^2}{m_H^2} \sqrt{-\Delta_H} \arctan\left(\frac{1}{\sqrt{-\Delta_H}}\right) \right] \right\}.
\end{aligned} \tag{44}$$

The above expression simplifies a lot in the limit of vanishing Higgs mass

$$\hat{\Sigma}_H(p^2) = \alpha_t p^2 \left[2\Delta_\chi \sqrt{-\Delta_\chi} \arctan\left(\frac{1}{\sqrt{-\Delta_\chi}}\right) - 2\Delta_\chi - \frac{2}{3} \right]. \tag{45}$$

The expression for the on-shell renormalized Higgs self-energy above the production threshold is given by

$$\begin{aligned}
\hat{\Sigma}_H(p^2) &= \alpha_t p^2 \left\{ \Delta_\chi \left\{ \frac{\sqrt{\Delta_\chi}}{2} \log \left[\frac{(1 + \sqrt{\Delta_\chi})p^2 - 2m_t^2}{(1 - \sqrt{\Delta_\chi})p^2 - 2m_t^2} \right] - 2\sqrt{-\Delta_H} \arctan\left(\frac{1}{\sqrt{-\Delta_H}}\right) - i\pi\sqrt{\Delta_\chi} \right\} \right. \\
&\quad \left. - \left(1 - \frac{m_H^2}{p^2}\right) \left[\Delta_H + \frac{4m_t^2}{m_H^2} \sqrt{-\Delta_H} \arctan\left(\frac{1}{\sqrt{-\Delta_H}}\right) \right] \right\}.
\end{aligned} \tag{46}$$

Also in this case, if we neglect the Higgs mass we obtain a simplified expression

$$\hat{\Sigma}_H(p^2) = \alpha_t p^2 \left\{ \frac{\Delta_\chi}{2} \sqrt{\Delta_\chi} \log \left[\frac{(1 + \sqrt{\Delta_\chi})p^2 - 2m_t^2}{(1 - \sqrt{\Delta_\chi})p^2 - 2m_t^2} \right] - 2\Delta_\chi - \frac{2}{3} - i\pi\Delta_\chi \sqrt{\Delta_\chi} \right\}. \tag{47}$$

The behavior of the renormalized self-energy for large momentum is

$$\begin{aligned}
\hat{\Sigma}_H(p^2) &= \alpha_t p^2 \left[\log\left(-\frac{p^2}{m_t^2} - i\epsilon\right) - \frac{8}{3} \right], \\
&\quad \text{for } p^2 \gg m_t^2, m_H^2.
\end{aligned} \tag{48}$$

The Dyson resummed Higgs propagator at the leading order in the large N_G limit is given by

$$\hat{D}_H(p^2) = \frac{i}{p^2 - m_H^2 - \hat{\Sigma}_H(p^2) + i\epsilon}. \quad (49)$$

Besides the real pole at $p^2 = m_H^2$ corresponding to the Higgs particle, the exact Higgs propagator in Eq. (49) contains a tachyon pole. Its Euclidean position, $p^2 = -\Lambda_{T,H}^2$, can be obtained by solving numerically the following equation:

$$\begin{aligned} & \left(1 + \frac{4}{\lambda_{T,H}^2}\right) \left\{ \sqrt{1 + \frac{4}{\lambda_{T,H}^2}} \log \left[\frac{\lambda_{T,H}^2 + 2 + \sqrt{\lambda_{T,H}^4 + 4\lambda_{T,H}^2}}{\lambda_{T,H}^2 + 2 - \sqrt{\lambda_{T,H}^4 + 4\lambda_{T,H}^2}} \right] - 4\sqrt{-\Delta_H} \arctan\left(\frac{1}{\sqrt{-\Delta_H}}\right) \right\} \\ & = \left(2 + \frac{m_H^2}{m_t^2} \frac{2}{\lambda_{T,H}^2}\right) \left[\frac{1}{\alpha_t} + \Delta_H + \frac{4m_t^2}{m_H^2} \sqrt{-\Delta_H} \arctan\left(\frac{1}{\sqrt{-\Delta_H}}\right) \right], \\ & \lambda_{T,H}^2 = \frac{\Lambda_{T,H}^2}{m_t^2}. \end{aligned} \quad (50)$$

In the zero Higgs mass limit the above equation simplifies and reads

$$\left(1 + \frac{4}{\lambda_{T,H}^2}\right) \left\{ \sqrt{1 + \frac{4}{\lambda_{T,H}^2}} \log \left[\frac{\lambda_{T,H}^2 + 2 + \sqrt{\lambda_{T,H}^4 + 4\lambda_{T,H}^2}}{\lambda_{T,H}^2 + 2 - \sqrt{\lambda_{T,H}^4 + 4\lambda_{T,H}^2}} \right] - 4 \right\} = \frac{2}{\alpha_t} + \frac{4}{3}. \quad (51)$$

The impact of a finite Higgs mass on the position of the tachyon can be quite sizable. Indeed, it turns out that with a finite Higgs mass, $m_H = 125$ GeV and $m_t = 172$ GeV as a reference top mass, $\lambda_{T,H}$ is about 6%–8% smaller than the same quantity with zero Higgs mass.

A crude estimation of the position of the tachyonic pole can be given by using the approximate expression in Eq. (48) instead of the full one

$$\Lambda_{T,H}^2 = m_t^2 \exp\left(\frac{1}{\alpha_t} + \frac{8}{3}\right). \quad (52)$$

In Fig. 8 we show a comparison between the exact position of the tachyon (divided by the top-quark mass) both for a massless Higgs boson and for $m_H = 125$ GeV and the approximated expression in the above equation. The latter nicely reproduces the exact result for $\alpha_t < 1$,

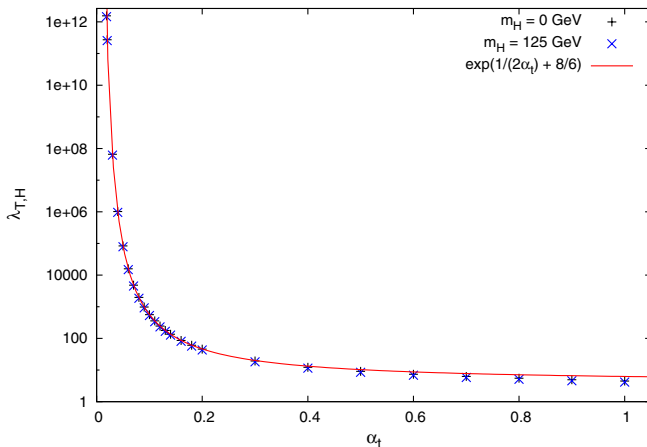


FIG. 8 (color online). Comparison between the exact result for $\lambda_{T,H}$ and its approximation.

while for bigger values of the coupling constant it starts overestimating it.

The residuum at the tachyon pole, κ_H , can be computed exactly in terms of $\lambda_{T,H}^2$ and of the ratio m_H^2/m_t^2 ,

$$\begin{aligned} \frac{1}{\kappa_H} &= 1 - \left(1 + \frac{m_H^2}{m_t^2} \frac{1}{\lambda_{T,H}^2}\right) \left\{ 1 + \alpha_t - \frac{6\alpha_t}{\lambda_{T,H}^2 + 4} \right. \\ & \quad \left. \times \left[\frac{1}{\alpha_t} + \Delta_H + \frac{4m_t^2}{m_H^2} \sqrt{-\Delta_H} \arctan\left(\frac{1}{\sqrt{-\Delta_H}}\right) \right] \right\}. \end{aligned} \quad (53)$$

In the limit of vanishing Higgs mass the above equation simplifies and reads

$$\frac{1}{\kappa_H} = -\alpha_t + \frac{4\alpha_t + 6}{\lambda_{T,H}^2 + 4}. \quad (54)$$

In the above equation $\lambda_{T,H}^2$ is the solution of Eq. (51) and not of the complete equation. We found that the impact of a finite Higgs mass on the residuum at the tachyonic pole is completely negligible. The opposite of the residuum, $-\kappa_H$, is plotted against α_t together with its approximation, $-\kappa_H = \frac{1}{\alpha_t}$ in Fig. 9.

The spectral representation of the Higgs propagator (49) is given by

$$\hat{D}_H(p^2) = \int_{-\infty}^{+\infty} ds \frac{i\rho^H(s)}{p^2 - s + i\epsilon}, \quad (55)$$

where $\rho^H(s) = \rho_T^H(s) + \delta(s - m_H^2) + \rho_+^H(s)\theta(s - 4m_t^2)$.

Notice that due to the tachyonic contribution to the spectral function,

$$\rho_T^H(s) = \kappa_H \delta(s + \Lambda_{T,H}^2), \quad (56)$$

the exact Higgs propagator (49) does not satisfy the usual Källén–Lehmann spectral representation. The other contribution to the spectral function, which comes from the positive part of the spectrum, is given by

$$\rho_+^H(s) = \frac{\alpha_t}{s} \frac{\Delta_\chi \sqrt{\Delta_\chi}}{\left\{ 1 - \alpha_t \left[\frac{\Delta_\chi}{2} \sqrt{\Delta_\chi} \log \left[\frac{(1 + \sqrt{\Delta_\chi})s - 2m_t^2}{(1 - \sqrt{\Delta_\chi})s - 2m_t^2} \right] - 2\Delta_\chi - \frac{2}{3} \right\]^2 + \pi^2 \alpha_t^2 \Delta_\chi^3} \right.} \quad (57)$$

The integral over the spectrum of ρ_+^H is convergent, since in the high-energy limit one has

$$\rho_+^H(s) \simeq \frac{\alpha_t}{s} \frac{1}{\left[1 - \alpha_t \log\left(\frac{s}{m_t^2}\right) + \frac{8}{3} \alpha_t \right]^2 + \pi^2 \alpha_t^2}. \quad (58)$$

In the above equations we have reported the positive part of the spectral function for a massless Higgs boson. The complete expression of ρ_+^H for a generic Higgs mass is rather cumbersome and can easily be obtained from Eq. (46).

Notice that also for the Higgs boson the integral over the spectrum is divergent order by order in perturbation theory. Indeed, by expanding ρ_+^H in powers of α_t , one finds, at the leading order, a function,

$$\rho_+^H(s) = \frac{\alpha_t}{s} \left(1 - \frac{4m_t^2}{s} \right) \sqrt{1 - \frac{4m_t^2}{s}} + O(\alpha_t^2), \quad (59)$$

which is not integrable over the positive part of the spectrum.

By using the residue theorem, one can prove that the integral over the whole spectrum of ρ^H vanishes (both for a massless and a massive Higgs boson)

$$\int_{-\infty}^{+\infty} ds \rho^H(s) = \kappa_H + 1 + \int_{4m_t^2}^{+\infty} ds \rho_+^H(s) = 0. \quad (60)$$

The above result has been confirmed by a careful numerical integration.

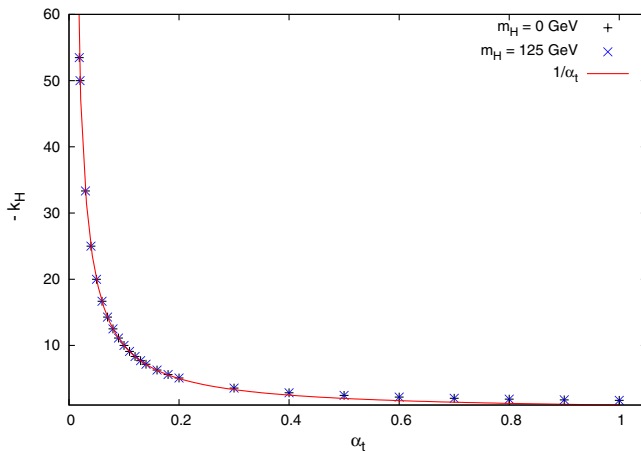


FIG. 9 (color online). Comparison between the exact result for $-\kappa_H$ and its approximation.

We propose to minimally subtract the tachyonic pole

$$\hat{D}_H^{\text{MS}}(p^2) = \frac{i}{p^2 - m_H^2 - \hat{\Sigma}_H(p^2) + i\epsilon} - \frac{i\kappa_H}{p^2 + \Lambda_{H,T}^2}. \quad (61)$$

Normalizing the spectral density amounts to rescaling the subtracted propagator by a factor $-\frac{1}{\kappa_H}$.

According to the bMS scheme the tachyon-subtracted propagator is given by

$$\hat{D}_H^{\text{bMS}}(p^2) = \frac{i}{p^2 - m_H^2 - \hat{\Sigma}_H(p^2) + i\epsilon} + \frac{i\kappa_H(\Lambda_{H,T}^2 + m_H^2)}{(p^2 - m_H^2)(p^2 + \Lambda_{H,T}^2)}. \quad (62)$$

Also here one removes the tachyon without modifying the normalization of the spectral function. One finds

$$\hat{D}_H^{\text{bMS}}(p^2) = \int_0^{+\infty} ds \frac{i\rho_{\text{bMS}}^H(s)}{p^2 - s + i\epsilon},$$

where $\rho_{\text{bMS}}^H(s) = (1 + \kappa_H)\delta(s - m_H^2) + \rho_+^H(s)\theta(s - 4m_t^2)$.

(63)

By using the nonminimal subtraction term in Eq. (62), one subtracts the tachyonic pole and adds its residuum to the Higgs pole at $p^2 = m_H^2$.

III. PERTURBATIVE AND NONPERTURBATIVE CONTRIBUTIONS TO THE ρ PARAMETER

The ρ parameter is usually defined as the ratio between the neutral and charged current coupling constants at zero momentum transfer

$$\rho = \frac{J_{\text{NC}}(0)}{J_{\text{CC}}(0)} = \frac{1}{1 - \Delta\rho}. \quad (64)$$

$J_{\text{CC}}(0)$ is given by the Fermi coupling constant, G_F , determined from the μ -decay rate, while $J_{\text{NC}}(0)$ can be measured in neutrino scattering on electrons or hadrons. Notice that this definition of the ρ parameter is process dependent since, in general, the radiative corrections depend on the hypercharge of the particles involved in the scattering process. However, the leading contributions in the top-quark mass to $\Delta\rho$ are universal.

At tree level the ρ parameter is given by $\rho = \frac{M_W^2}{M_Z^2 c_W^2} = 1$. At the leading order in the top-quark mass, radiative corrections to ρ can be obtained from the wave function renormalization of the unphysical scalars. Let us consider the kinetic terms of the scalar part of the SM Lagrangian.

The UV divergences that show up in radiative corrections can be reabsorbed by introducing suitable wave function renormalization constants in the following way:

$$\mathcal{L}_{\text{KS}} = Z_\phi \left| \partial_\mu \phi^- + i \frac{g\nu}{2} W_\mu^- \right|^2 + \frac{Z_\chi}{2} \left(\partial_\mu \chi + \frac{g\nu}{2c_W} Z_\mu \right)^2 + \text{other terms.} \quad (65)$$

The renormalized masses of the gauge bosons are given by

$$M_W = \sqrt{Z_\phi} \frac{g\nu}{2}, \quad M_Z = \sqrt{Z_\chi} \frac{g\nu}{2c_W}, \quad \text{thus } \rho = \frac{Z_\phi}{Z_\chi}. \quad (66)$$

The one-loop wave function renormalization constants of the unphysical scalars have been computed in the previous section; see Eqs. (3) and (23). By using these results, we immediately get the standard one-loop top contribution to the ρ parameter

$$\Delta\rho_p = \frac{\alpha_t}{2} + O(\alpha_t^2) = \frac{\sqrt{2}}{16\pi^2} N_c N_G G_F m_t^2 + O(G_F^2 m_t^4). \quad (67)$$

Our resummation and subsequent tachyonic subtraction of the scalar propagators allows us to give an estimate of the nonperturbative leading top-mass contribution to the ρ parameter.

The residuum at the tachyon pole, κ , can be viewed as the contribution from the continuous part of the spectrum to the wave function renormalization constants; see Eqs. (19), (39), and (65). Therefore, according to the bMS scheme, one has

$$Z_\chi = \frac{1}{1 + \kappa_\chi}, \quad Z_\phi = \frac{1}{1 + \kappa_\phi} \Rightarrow \Delta\rho_c = 1 - \frac{1 + \kappa_\phi}{1 + \kappa_\chi}. \quad (68)$$

It is worth noticing that the continuous contribution to $\Delta\rho$ is always negative with this prescription. Moreover its absolute value slowly increases with α_t .

It is interesting to compare the bMS approach with the Akhoury scheme. In this case we find, by normalizing the spectral densities with a constant factor, the following result:

$$Z_\chi = -\kappa_\chi, \quad Z_\phi = -\kappa_\phi \Rightarrow \Delta\rho_c = 1 - \frac{\kappa_\chi}{\kappa_\phi}. \quad (69)$$

In the Akhoury scheme the continuous contribution to $\Delta\rho$ is positive, it grows with α_t until it reaches its maximum value, $\Delta\rho_c \simeq 0.038$, for $\alpha_t \simeq 1$, and eventually it starts decreasing. We notice that the behavior in the two schemes is quite different. This reflects the uncertainties in the definition of resummation in improved perturbation theory. The Akhoury scheme appears to be more in agreement with the idea that the improvement of perturbation theory through the summation of the renormalon chain should act as a cutoff of the theory. The results of the bMS-like calculation are hard to interpret physically. We notice that the bMS scheme in this case is not as well motivated as in QCD, where asymptotic freedom acts as an additional guiding principle.

IV. TOP PROPAGATOR

In this section we discuss the one-loop self-energy corrections to the top-quark propagator and their renormalization in the on-shell scheme. It turns out that all the contributing graphs are of order $O(1)$ in the large N_G limit. We select a gauge invariant subset of self-energy amplitudes by considering the limit of vanishing gauge coupling constants, i.e. $g, g' \rightarrow 0$. Indeed, in this approximation, which amounts to neglecting the vector boson masses with respect to (w.r.t.) the Higgs boson and the top-quark masses, one is left with the Feynman graphs depicted in Fig. 10.

The contribution of graph 1 is given by (for the notation see Appendix B)

$$i\sqrt{2}G_F m_t^2 \left[(\not{p} + m_t) \int_0^{+\infty} ds \rho_{\text{phy}}^H(s) B_0[p^2, \sqrt{s}, m_t] - \not{p} \int_0^{+\infty} ds \rho_{\text{phy}}^H(s) B_1[p^2, \sqrt{s}, m_t] \right], \quad (70)$$

where $\rho_{\text{phy}}^H(s) = \delta(s - m_H^2) + \rho_+^H(s)\theta(s - 4m_t^2)$ is the physical, subtracted spectral function. Therefore, one finds a contribution from the Higgs pole, which is just the one-loop amplitude, and a contribution from the continuous part of the spectrum.

Some comments are in order. (i) Both the scalar and the rank one tensor two-point functions in the above equation, i.e. $B_0[p^2, \sqrt{s}, m_t]$ and $B_1[p^2, \sqrt{s}, m_t]$, respectively, have a physical threshold at $p^2 = (\sqrt{s} + m_t)^2$. Since the continuous part of the spectrum starts at $\sqrt{s} = 2m_t$, the contribution of the latter to the self-energy contains an imaginary part only for $p^2 > 9m_t^2$. (ii) The integral of the imaginary part is convergent being over a compact domain, namely $4m_t^2 < s < (\sqrt{p^2} - m_t)^2$. (iii) The integral over the spectrum of the real part of the two-point functions in Eq. (70) does not converge. In order to see this, we can limit ourselves to the case $p^2 \leq (\sqrt{s} - m_t)^2$, for the remaining parts of the integrals, if any, are convergent being over a compact domain. By using Eqs. (B10) and (B14), one can show that at the leading order in the limit $s \gg p^2, m_t^2$, Eq. (70) reads

$$\frac{\sqrt{2}}{16\pi^2} G_F m_t^2 \left\{ (\not{p} + m_t) \int_0^{+\infty} ds \rho_+^H(s) \left[\frac{2}{D-4} + 1 + \log\left(\frac{s}{\Lambda_B^2}\right) \right] - \frac{\not{p}}{2} \int_0^{+\infty} ds \rho_+^H(s) \left[\frac{2}{D-4} + \frac{1}{2} + \log\left(\frac{s}{\Lambda_B^2}\right) \right] \right\}. \quad (71)$$

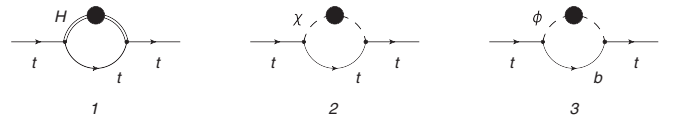


FIG. 10. Top-quark self-energy at one loop in the gaugeless limit. The lines with a bubble denote a resummed scalar propagator.

Both integrals in the above equation are logarithmically divergent.

The previous considerations suggest that the on-shell renormalization of the top-quark self-energy, besides removing the poles in $D - 4$, improves also the behavior of the integrals over s . This is indeed the case. In fact, in the limit where $s \gg p^2, m_t^2$, the subtracted two-point functions go to zero as $1/s$,

$$\begin{aligned} DB_0[p^2, \sqrt{s}, m_t] &:= B_0[p^2, \sqrt{s}, m_t] - \text{Re}(B_0[p^2 = m_t^2, \sqrt{s}, m_t]) \\ &= \frac{m_t^2 - p^2}{2s} + O\left(\frac{1}{s^2}\right), \\ DB_1[p^2, \sqrt{s}, m_t] &:= B_1[p^2, \sqrt{s}, m_t] - \text{Re}(B_1[p^2 = m_t^2, \sqrt{s}, m_t]) \\ &= \frac{m_t^2 - p^2}{3s} + O\left(\frac{1}{s^2}\right). \end{aligned} \quad (72)$$

This behavior entails that the integral over the positive part of the spectrum of the subtracted functions in Eq. (72) multiplied by $\rho_+^H(s)$ is convergent and can be computed numerically.

We now move to the contribution of the second graph in Fig. 10,

$$\begin{aligned} i\sqrt{2}G_F m_t^2 \left[(\not{p} - m_t) \int_0^{+\infty} ds \rho_{\text{phy}}^X(s) B_0[p^2, \sqrt{s}, m_t] \right. \\ \left. - \not{p} \int_0^{+\infty} ds \rho_{\text{phy}}^X(s) B_1[p^2, \sqrt{s}, m_t] \right], \end{aligned} \quad (73)$$

where $\rho_{\text{phy}}^X(s) = \delta(s) + \rho_+^X(s)\theta(s - 4m_t^2)$ is the physical, subtracted spectral function. Thus, one finds a contribution from the massless Goldstone pole, which is just the one-loop amplitude, and a contribution from the continuous part of the spectrum. The latter coincides, a part for the spectral function and the sign of the mass term, with the continuous contribution to the top-Higgs bubble in Eq. (70).

Finally, we report here the expression of the third graph in Fig. 10 in the limit of vanishing bottom mass

$$\begin{aligned} 2i\sqrt{2}G_F m_t^2 \not{p} \omega_+ \int_0^{+\infty} ds \rho_{\text{phy}}^\phi(s) (B_0[p^2, \sqrt{s}, 0] \\ - B_1[p^2, \sqrt{s}, 0]), \end{aligned} \quad (74)$$

where $\rho_{\text{phy}}^\phi(s) = \delta(s) + \rho_+^\phi(s)\theta(s - m_t^2)$ is the physical, subtracted spectral function, while $\omega_+ = \frac{1+\gamma_5}{2}$ is the positive chirality projector. Also in this case, one finds a contribution from the massless Goldstone pole, which is just the one-loop amplitude, and a contribution from the continuous part of the spectrum. Arguments similar to those presented for the top-Higgs bubble allow us to conclude that the continuous contribution to the self-energy coming from the bottom- ϕ bubble contains an imaginary part for $p^2 > m_t^2$. The on-shell renormalization of the self-energy amplitude in Eq. (74) guarantees the convergence of the integral over the positive part of the spectrum. Indeed, in the limit where $s \gg p^2, m_t^2$, one finds

$$2(DB_0[p^2, \sqrt{s}, 0] - DB_1[p^2, \sqrt{s}, 0]) = \frac{m_t^2 - p^2}{3s} + O\left(\frac{1}{s^2}\right). \quad (75)$$

It is convenient to parametrize the top-quark self-energy, $\hat{\Sigma}_t(p)$, by means of momentum and mass form factors according to the following definition:

$$\begin{aligned} \hat{\Sigma}_t(p) = \frac{\sqrt{2}}{16\pi^2} G_F m_t^2 [(a_+^{ll}(p^2) + a_+^c(p^2, \alpha_t)) \not{p} \omega_+ \\ + (a_-^{ll}(p^2) + a_-^c(p^2, \alpha_t)) \not{p} \omega_- + (a_m^{ll}(p^2) \\ + a_m^c(p^2, \alpha_t)) m_t], \end{aligned} \quad (76)$$

where the coefficients a_+ , a_- , and a_m are given by

$$\begin{aligned} a_+^{ll}(p^2) &= \frac{16\pi^2}{-i} (DB_0[p^2, m_H, m_t] - DB_1[p^2, m_H, m_t] + DB_0[p^2, 0, m_t] - DB_1[p^2, 0, m_t]) \\ &\quad + \frac{32\pi^2}{-i} (DB_0[p^2, 0, 0] - DB_1[p^2, 0, 0]), \\ a_+^c(p^2, \alpha_t) &= \frac{16\pi^2}{-i} \int_{4m_t^2}^{+\infty} ds (\rho_+^H(s) + \rho_+^X(s)) (DB_0[p^2, \sqrt{s}, m_t] - DB_1[p^2, \sqrt{s}, m_t]) \\ &\quad + \frac{32\pi^2}{-i} \int_{m_t^2}^{+\infty} ds \rho_+^\phi(s) (DB_0[p^2, \sqrt{s}, 0] - DB_1[p^2, \sqrt{s}, 0]), \\ a_-^{ll}(p^2) &= \frac{16\pi^2}{-i} (DB_0[p^2, m_H, m_t] - DB_1[p^2, m_H, m_t] + DB_0[p^2, 0, m_t] - DB_1[p^2, 0, m_t]), \\ a_-^c(p^2, \alpha_t) &= \frac{16\pi^2}{-i} \int_{4m_t^2}^{+\infty} ds (\rho_+^H(s) + \rho_+^X(s)) (DB_0[p^2, \sqrt{s}, m_t] - DB_1[p^2, \sqrt{s}, m_t]), \\ a_m^{ll}(p^2) &= \frac{16\pi^2}{-i} (DB_0[p^2, m_H, m_t] - DB_0[p^2, 0, m_t]), \\ a_m^c(p^2, \alpha_t) &= \frac{16\pi^2}{-i} \int_{4m_t^2}^{+\infty} ds (\rho_+^H(s) - \rho_+^X(s)) DB_0[p^2, \sqrt{s}, m_t]. \end{aligned} \quad (77)$$

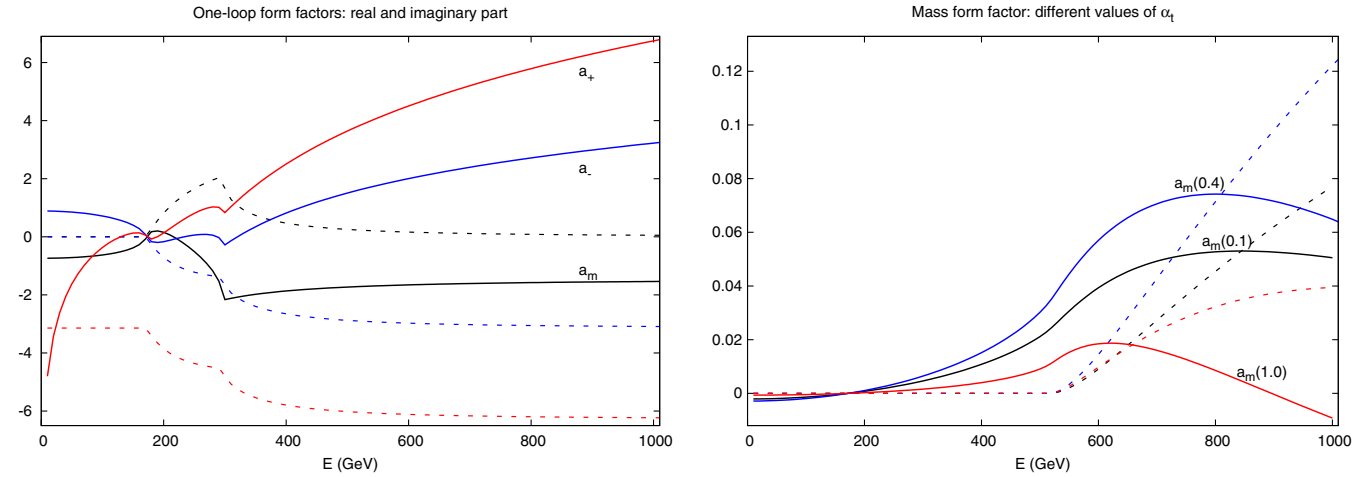


FIG. 11 (color online). Left panel: real (solid lines) and imaginary (dashed lines, same colors) parts of the one-loop form factors. Right panel: real (solid lines) and imaginary (dashed lines) parts of the continuous contribution to the mass form factor for three values of α_t .

In Fig. 11 (left panel) we plot the real (solid lines) and imaginary (dashed lines) parts of the one-loop form factors as functions of the external momentum, $\sqrt{p^2}$. The presence of two thresholds at $\sqrt{p^2} = m_t \approx 170$ GeV and $\sqrt{p^2} = m_t + m_H \approx 300$ GeV is clearly distinguishable. In the right panel of the same figure we show the behavior of the real (solid lines) and imaginary (dashed lines) parts of the continuous contribution to the mass form factor for different values of the coupling constant α_t . The real part of $\alpha_m^c(p^2, \alpha_t)$ as a function of the external momentum has a maximum that depends on α_t , though it is always located beyond the threshold at $\sqrt{p^2} = 3m_t = 516$ GeV. The impact of the continuous part of the spectrum on the mass form factor is negligible ($< 5\%$) over the whole range of momentum considered. In Fig. 12 the continuous contribution to the real (solid lines) and imaginary (dashed lines) parts of the momentum form factors with negative (left panel) and positive (right panel) chirality is plotted as a function of the

external momentum for different values of α_t . It turns out that in this case the continuous contribution to the momentum form factors can be a sizable fraction (5%–10%) of the corresponding one-loop contribution for $\sqrt{p^2} > 500$ GeV. A detailed inspection shows that the effects of the continuous part of the spectrum on all form factors grow with α_t until they reach their maximum for $\alpha_t \approx 0.4$ and then they decrease. Finally, in Fig. 13 we present a comparison between the real (left panel) and the imaginary (right panel) parts of the continuous contribution to the form factors computed with a finite Higgs mass (solid lines), namely $m_H = 125$ GeV, and in the approximation of vanishing Higgs mass (dashed lines). A fixed value of the coupling constant, $\alpha_t = 0.4$, has been used to compute all the form factors. One can see that the impact of a finite Higgs mass is small ($< 5\%$) on the momentum form factors, but can be quite big (around 20%–25% for $\sqrt{p^2} < 700$ GeV and bigger than 30% for $\sqrt{p^2} > 800$ GeV) on the mass form factor.

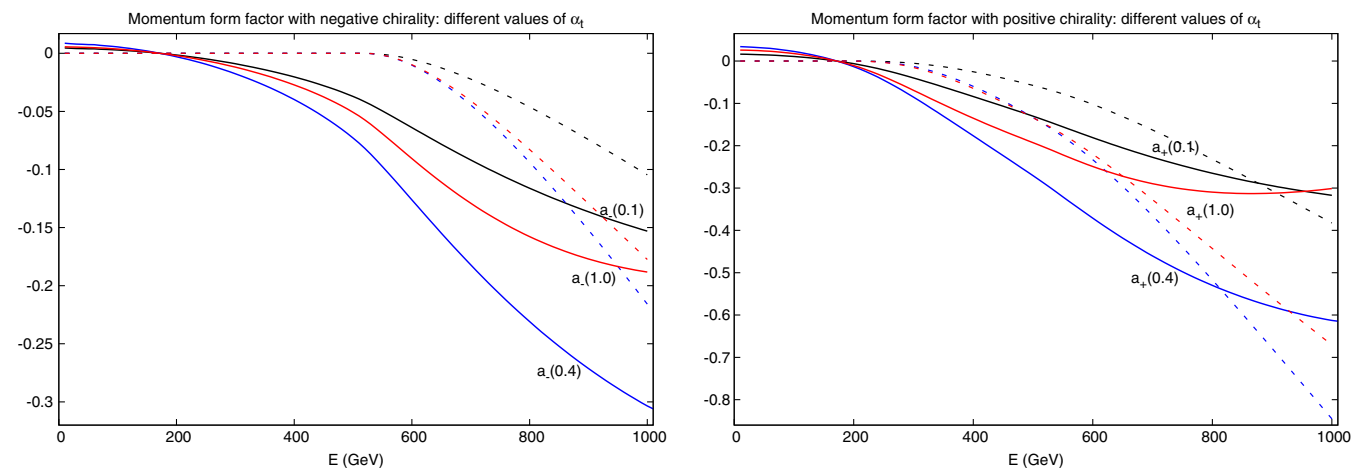


FIG. 12 (color online). Left panel: real (solid lines) and imaginary (dashed lines, same colors) parts of the continuous contribution to the momentum form factor with negative chirality for three values of α_t . Right panel: same plot, but with positive chirality.

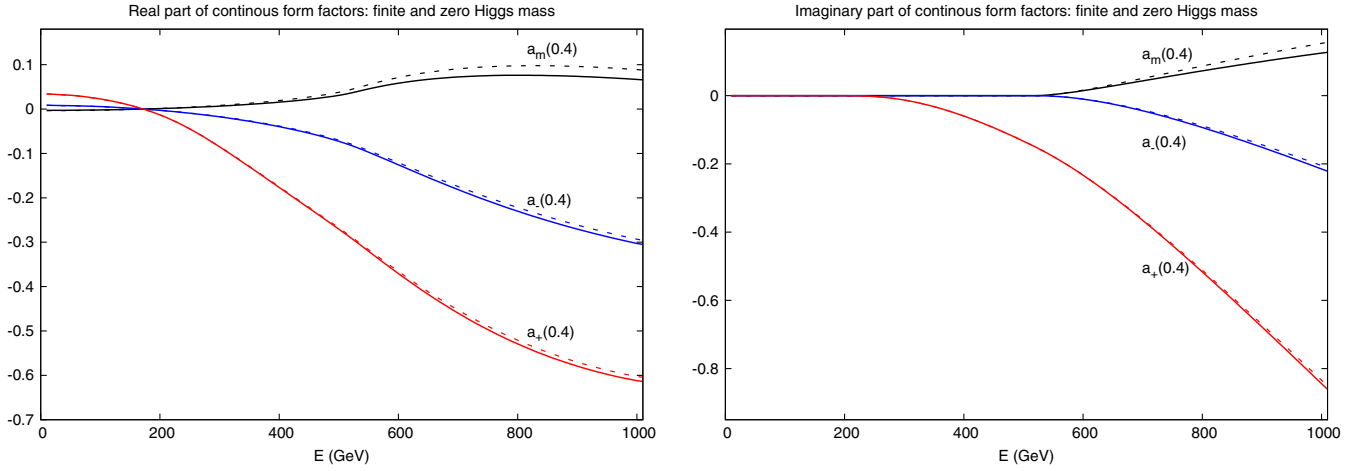


FIG. 13 (color online). Left panel: real parts of the continuous contribution to the form factors computed with $m_H = 125$ GeV (solid lines) and with $m_H = 0$ GeV (dashed lines). Right panel: same plot with the imaginary parts.

Complex pole of the top propagator

In this subsection we compute the complex pole of the Dyson resummed top propagator and extract from it the width of the top quark. Moreover, the impact on this latter quantity of the continuous part of the spectrum is estimated.

The Dyson resummed top propagator,

$$\Delta_t(p) = \frac{i}{\not{p} - m_t - \hat{\Sigma}_t(p) + i\epsilon}, \quad (78)$$

can be cast in the following form:

$$\Delta_t(p) = \frac{i}{D(p^2)} \left[\frac{\not{p}\omega_+}{1 - \tilde{a}_-(p^2, \alpha_t)} + \frac{\not{p}\omega_-}{1 - \tilde{a}_+(p^2, \alpha_t)} + \frac{m_t(1 + \tilde{a}_m(p^2, \alpha_t))}{(1 - \tilde{a}_-(p^2, \alpha_t))(1 - \tilde{a}_+(p^2, \alpha_t))} \right], \quad (79)$$

where

$$D(p^2) = p^2 - m_t^2 \frac{(1 + \tilde{a}_m(p^2, \alpha_t))^2}{(1 - \tilde{a}_-(p^2, \alpha_t))(1 - \tilde{a}_+(p^2, \alpha_t))}. \quad (80)$$

The form factors appearing in the above equations are given by the rescaled sum of the one-loop and the continuous form factors given in Eq. (77), i.e.

TABLE I. Top quark's width expressed in GeV.

M_t	$\Gamma_t^{1l}(m_H = 125)$	$\Gamma_t^{1l+\text{cont}}(m_H = 125)$	$\Gamma_t^{1l}(m_H = 0)$	$\Gamma_t^{1l+\text{cont}}(m_H = 0)$
172	1.6666	1.6666	1.6670	1.6670
200	1.8286	1.8286	3.7368	3.7367
300	2.8969	2.9077	8.2406	8.2510
400	9.4270	9.4977	11.6188	11.6894
500	13.2124	13.4136	14.7659	14.9677
600	16.6049	16.9956	17.8448	18.2295
700	19.8499	20.5433	20.8998	21.5559
800	23.0236	24.1733	23.9460	25.0080
900	26.1581	27.9215	26.9893	28.6014
1000	29.2691	31.8017	30.0325	32.3400
1100	32.3649	35.8185	33.0767	36.2235
1200	35.4509	39.9722	36.1224	40.2493
1300	38.5300	44.2607	39.1699	44.4138
1400	41.6046	48.6807	42.2194	48.7126
1500	44.6758	53.2280	45.2707	53.1409
1600	47.7449	57.8979	48.3240	57.6941
1700	50.8124	62.6856	51.3791	62.3670
1800	53.8790	67.5863	54.4360	67.1549
1900	56.9449	72.5950	57.4945	72.0528
2000	60.0106	77.7069	60.5548	77.0560

$$\tilde{a}_i(p^2, \alpha_i) = \frac{\sqrt{2}}{16\pi^2} G_F m_t^2 [a_i^{ll}(p^2) + a_i^c(p^2, \alpha_i)],$$

$$i = +, -, m.$$

The pole of the resummed propagator, s , which in general is a complex quantity, can be obtained by solving numerically the following equation:

$$\frac{s}{m_t^2} = \frac{(1 + \tilde{a}_m(s, \alpha_t))^2}{(1 - \tilde{a}_-(s, \alpha_t))(1 - \tilde{a}_+(s, \alpha_t))}. \quad (81)$$

We parametrize the complex pole s in the following way:

$$\sqrt{s} = M_t - \frac{i}{2}\Gamma_t, \quad (82)$$

where M_t is the physical top mass and Γ_t its width. In this way, neglecting quadratic corrections in the width (narrow width approximation), one finds $s = M_t^2 - iM_t\Gamma_t$.

In Table I we show the width of the top quark, Γ_t , as a function of its physical mass, M_t . In particular, we compare results obtained by taking into account one-loop corrections to the top propagator only, with those where the contribution coming from the continuous part of the spectrum has been added. It turns out that the impact of nonperturbative corrections on the top width is small ($< 7\%$) for $M_t < 1$ TeV, but becomes quite sizable ($> 15\%$) for heavier masses, typically above 1.5 TeV. Finally, our results show that the presence of a light Higgs boson, with mass $m_H = 125$ GeV, affects the width of the top-quark significantly ($> 10\%$) only if the latter is light, $M_t < 500$ GeV.

V. BOTTOM PROPAGATOR

In this section we discuss the one-loop self-energy corrections to the bottom-quark propagator and their renormalization in the on-shell scheme. It turns out that all the contributing graphs are of order $O(1)$ in the large- N_G limit. We select a gauge invariant subset of self-energy

amplitudes by considering the limit where $g, g' \rightarrow 0$. The resulting graphs can be obtained from those depicted in Fig. 10 by substituting a top propagator with a bottom one and vice versa.

The contribution of graphs 1 and 2 to the bottom self-energy, $\Sigma_b(p)$, is proportional to $G_F m_b^2$, and thus it can be neglected. The expression of the third graph is given by

$$2i\sqrt{2}G_F m_t^2 \not{p}\omega_- \int_0^{+\infty} ds \rho_{\text{phy}}^\phi(s) (B_0[p^2, \sqrt{s}, m_t] - B_1[p^2, \sqrt{s}, m_t]). \quad (83)$$

In the above equation one finds a contribution from the massless Goldstone pole, which is just the one-loop amplitude and a contribution from the continuous part of the spectrum. The latter has a physical threshold, above which an imaginary part shows up, at $p^2 = 4m_t^2$ due to the fact that the continuous part of the spectrum starts at $\sqrt{s} = m_t$. Moreover, the on-shell renormalization of the bottom self-energy in Eq. (83) guarantees the convergence of the integral over the positive part of the spectrum.

It is convenient to parametrize the bottom-quark self-energy, $\hat{\Sigma}_b(p)$, by means of a momentum form factor according to the following definition:

$$\hat{\Sigma}_b(p) = \frac{\sqrt{2}}{16\pi^2} G_F m_t^2 (b_-^{ll}(p^2) + b_-^c(p^2, \alpha_t)) \not{p}\omega_-, \quad (84)$$

where the coefficients are given by

$$b_-^{ll}(p^2) = \frac{32\pi^2}{-i} (DB_0[p^2, 0, m_t] - DB_1[p^2, 0, m_t]),$$

$$b_-^c(p^2, \alpha_t) = \frac{32\pi^2}{-i} \int_{m_t^2}^{+\infty} ds \rho_+^\phi(s) (DB_0[p^2, \sqrt{s}, m_t] - DB_1[p^2, \sqrt{s}, m_t]). \quad (85)$$

In the left panel of Fig. 14 we show the real (solid line) and imaginary (dashed line) part of the one-loop

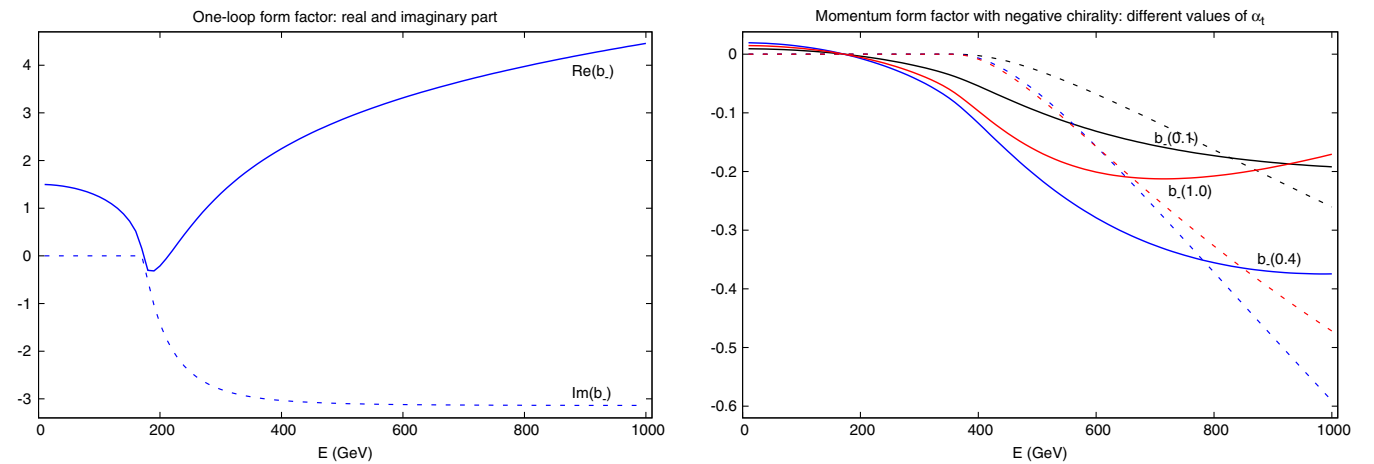


FIG. 14 (color online). Left panel: real (solid line) and imaginary (dashed line) part of the one-loop form factor. Right panel: real (solid lines) and imaginary (dashed lines, same colors) parts of the continuous contribution to the momentum form factor for three values of α_t .

momentum form factor of the bottom propagator. In the right panel of the same figure we plot the real (solid lines) and imaginary (dashed lines) parts of the continuous contribution to b_- for three different values of α_t . It turns out that the impact of the continuous part of the spectrum on the momentum form factor is not negligible, being about 5%–10% of the one-loop contribution for $\sqrt{p^2} > 500$ GeV. Finally, also in the case of the bottom propagator the effect of the continuous part of the spectrum on the form factor reaches its maximum for $\alpha_t \simeq 0.4$.

VI. CONCLUSION

The question whether the presence of a Landau pole, i.e. a tachyon pole in the propagator, signifies the breakdown of a theory or whether it is an artifact of perturbation theory is a difficult question. It has been with us for 60 years and one still cannot claim that the problem is solved. Within QCD analytic perturbation theory appears to give fundamentally correct results; however, here one uses asymptotic freedom as an essential subsidiary principle. In this paper we attempted to resum perturbation theory in a similar method by at least first subtracting the tachyon and subsequently calculate with the corrected propagator. We showed that such calculations are feasible in the electroweak sector. We focused on effects of a heavy top quark, which simplifies the discussion considerably, since the problems then appear in one place in the theory only and can be studied in isolation. Also the heavy top effects are the largest in the SM; however, perturbation theory is surely sufficient for the physical top-quark mass. Nonetheless the calculations are important for possible effects of a (very unlikely) fourth family or effects from fermion doubles, when one tries to take the continuum limit of a lattice action.

Lacking the extra input from asymptotic freedom, one needs new principles in order to constrain the uncertainties coming from nonperturbative effects. Following a previous paper in Higgs physics, we introduced the Akhoury scheme, which appears to give sensible results. The scheme was motivated by principles from renormalization theory like the normalization of the spectral density integral. An attempt to generalize analytic perturbation theory gave quite different results that do not look very meaningful. However, since rigorous principles constraining the treatment of nonperturbative uncertainties are missing in the electroweak case, we cannot come to a definite conclusion. It would be very useful if cutoff effects could be studied in an entirely different nonperturbative scheme, for instance, with a lattice Lagrangian. However, at the moment it appears unclear how one should put a chiral model with a heavy top quark and a massless bottom quark on the lattice. In particular, the fermion doubling problem will complicate things here due to the lack of (perturbative) decoupling of heavy fermion doubles.

ACKNOWLEDGMENTS

This work is supported by the DFG Project “(Nicht-)perturbative Quantenfeldtheorie.”

APPENDIX A: TREE-LEVEL LAGRANGIAN

For completeness we report here the Lagrangian that has been used in the computations. We have adopted a Landau gauge fixing in order to have massless would-be Goldstone bosons. We omit the vertices with three and four gauge fields, the ghost part of the Lagrangian, and all the fermion fields except the top and bottom quarks since they do not play a role in our computation. The bilinear part of the Lagrangian is given by

$$\begin{aligned} \mathcal{L}_{\text{bil}} = & W_\mu^+ g^{\mu\nu} (\square + M_W^2) W_\nu^- + \frac{1}{2} Z_\mu g^{\mu\nu} (\square + M_Z^2) Z_\nu + \frac{1}{2} A_\mu g^{\mu\nu} \square A_\nu - \phi^+ \square \phi^- - \frac{1}{2} H (\square + m_H^2) H \\ & - \frac{1}{2} \chi \square \chi + \sum_{k=1}^{N_G} [\bar{t}_k (i\not{\partial} - m_t) t_k + \bar{b}_k i\not{\partial} b_k], \end{aligned} \quad (\text{A1})$$

where $M_W = \frac{1}{2} g v$, $M_Z = \frac{M_W}{c_w}$, $m_H = \frac{1}{\sqrt{2}} \sqrt{\lambda} v$, and $m_t = \frac{1}{\sqrt{2}} y_t v$ and A_μ is the photon field.

The trilinear part of the Lagrangian is given by

$$\begin{aligned} \mathcal{L}_{\text{tri}} = & \frac{i}{2} g W_\mu^+ [\phi^- (\partial^\mu H + i\partial^\mu \chi) - (H + i\chi) \partial^\mu \phi^-] + \frac{i}{2} g W_\mu^- [(H - i\chi) \partial^\mu \phi^+ - \phi^+ (\partial^\mu H - i\partial^\mu \chi)] \\ & + \frac{i}{2} g Z_\mu (\phi^- \partial^\mu \phi^+ - \phi^+ \partial^\mu \phi^- + i\chi \partial^\mu H - iH \partial^\mu \chi) + \frac{1}{4} g^2 v H (2W^+ \cdot W^- + Z^2) \\ & - \frac{1}{4} \lambda v (H^3 + H\chi^2 + 2H\phi^+ \phi^-) + \frac{1}{\sqrt{2}} g \sum_{k=1}^{N_G} (\bar{t}_k W^+ \omega_- b_k + \bar{b}_k W^- \omega_- t_k) + \frac{1}{2} g \sum_{k=1}^{N_G} (\bar{t}_k Z \omega_- t_k - \bar{b}_k Z \omega_- b_k) \\ & + y_t \sum_{k=1}^{N_G} (\phi^+ \bar{t}_k \omega_- b_k + \phi^- \bar{b}_k \omega_+ t_k) - \frac{1}{\sqrt{2}} y_t \sum_{k=1}^{N_G} (H \bar{t}_k t_k - i\chi \bar{t}_k \gamma_5 t_k). \end{aligned} \quad (\text{A2})$$

Finally the quadrilinear part of the Lagrangian is given by

$$\begin{aligned} \mathcal{L}_{\text{quad}} = & \frac{1}{8} g^2 (2W^+ \cdot W^- + Z^2) (2\phi^+ \phi^- + H^2 + \chi^2) \\ & - \frac{1}{16} \lambda [4(\phi^+ \phi^-)^2 + H^4 + \chi^4 + 4\phi^+ \phi^- H^2 \\ & + 4\phi^+ \phi^- \chi^2 + 2H^2 \chi^2]. \end{aligned} \quad (\text{A3})$$

We remark that in the above equations all the mass parameters, the coupling constants, and the fields are bare quantity, even though a subscript ‘‘0’’ has not been added in order to avoid a cumbersome notation.

APPENDIX B: ONE-LOOP SCALAR INTEGRALS

We collect in this Appendix some useful formulas that have been used in this work. We denote with μ the mass scale introduced with dimensional regularization. Given the following definitions (with n a positive integer):

$$\begin{aligned} A_0^{(n)}[m] &= \int \frac{d^D q}{(2\pi)^D} \frac{\mu^{(4-D)}}{(q^2 - m^2 + i\epsilon)^n}, \\ B_0[p^2, m, M] &= \int \frac{d^D q}{(2\pi)^D} \frac{\mu^{(4-D)}}{(q^2 - m^2 + i\epsilon)[(q-p)^2 - M^2 + i\epsilon]}, \end{aligned} \quad (\text{B1})$$

it is straightforward to derive the explicit expression for the one-point functions $A_0^{(n)}$,

$$\begin{aligned} A_0^{(1)}[m] &\equiv A_0[m] = \frac{i}{(4\pi)^2} m^2 \left[\frac{2}{4-D} - 1 - \log\left(\frac{m^2}{\Lambda_B^2}\right) \right], \\ A_0^{(2)}[m] &= \frac{i}{(4\pi)^2} \left[\frac{2}{4-D} - 2 - \log\left(\frac{m^2}{\Lambda_B^2}\right) \right], \\ A_0^{(n)}[m] &= \frac{(-)^n i}{(4\pi)^2} \frac{1}{(n-2)(n-1)} \frac{1}{m^{2(n-2)}}, \quad \text{for } n > 2, \end{aligned} \quad (\text{B2})$$

where $\Lambda_B^2 = 4\pi\mu^2 \exp(2 - \gamma_E)$.

Before dealing with the complete expression of the scalar two-point function B_0 , we consider some special cases. We start with the simplest case, the one with two massless particle,

$$B_0[p^2, 0, 0] = \frac{i}{(4\pi)^2} \left[\frac{2}{4-D} - \log\left(-\frac{p^2}{\Lambda_B^2} - i\epsilon\right) \right]. \quad (\text{B3})$$

The two-point function in the case of one massive particle and one massless particle is given by

$$\begin{aligned} B_0[p^2, m, 0] &= \frac{i}{(4\pi)^2} \left[\frac{2}{4-D} - \log\left(\frac{m^2}{\Lambda_B^2}\right) \right. \\ &\quad \left. - \left(1 - \frac{m^2}{p^2}\right) \log\left(1 - \frac{p^2}{m^2}\right) \right]. \end{aligned} \quad (\text{B4})$$

The above expression is valid in the kinematical region $p^2 < m^2$, while above the production threshold, $p^2 > m^2$, we have

$$\begin{aligned} B_0[p^2, m, 0] &= \frac{i}{(4\pi)^2} \left[\frac{2}{4-D} - \log\left(\frac{m^2}{\Lambda_B^2}\right) - \left(1 - \frac{m^2}{p^2}\right) \right. \\ &\quad \left. \times \log\left(\frac{p^2}{m^2} - 1\right) + i\pi \left(1 - \frac{m^2}{p^2}\right) \right]. \end{aligned} \quad (\text{B5})$$

By using Eq. (B4) it is easy to prove that

$$\begin{aligned} \lim_{p^2 \rightarrow 0} B_0[p^2, m, 0] &= \frac{1}{m^2} A_0[m] \\ &= \frac{i}{(4\pi)^2} \left[\frac{2}{4-D} - 1 - \log\left(\frac{m^2}{\Lambda_B^2}\right) \right]. \end{aligned} \quad (\text{B6})$$

The two-point function in the case of two massive particles with equal mass below the production threshold, $p^2 < 4m^2$, reads

$$\begin{aligned} B_0[p^2, m, m] &= \frac{i}{(4\pi)^2} \left[\frac{2}{4-D} - \log\left(\frac{m^2}{\Lambda_B^2}\right) \right. \\ &\quad \left. - 2\sqrt{-\Delta} \arctan\left(\frac{1}{\sqrt{-\Delta}}\right) \right], \end{aligned} \quad (\text{B7})$$

where we have introduced the shorthand notation $\Delta = 1 - \frac{4m^2}{p^2}$. The two-point function with equal masses for $p^2 > 4m^2$ is given by

$$\begin{aligned} B_0[p^2, m, m] &= \frac{i}{(4\pi)^2} \left\{ \frac{2}{4-D} - \log\left(\frac{m^2}{\Lambda_B^2}\right) \right. \\ &\quad \left. - \frac{1}{2} \sqrt{\Delta} \log\left[\frac{(1 + \sqrt{\Delta})p^2 - 2m^2}{(1 - \sqrt{\Delta})p^2 - 2m^2} \right] + i\pi \sqrt{\Delta} \right\}. \end{aligned} \quad (\text{B8})$$

By using Eq. (B7) it is easy to prove that

$$\begin{aligned} \lim_{p^2 \rightarrow 0} B_0[p^2, m, m] &= A_0^{(2)}[m] \\ &= \frac{i}{(4\pi)^2} \left[\frac{2}{4-D} - 2 - \log\left(\frac{m^2}{\Lambda_B^2}\right) \right]. \end{aligned} \quad (\text{B9})$$

The two-point function in the general case of two different masses reads

$$\begin{aligned} B_0[p^2, m, M] &= \frac{i}{(4\pi)^2} \left\{ \frac{2}{4-D} - \log\left(\frac{m^2}{\Lambda_B^2}\right) \right. \\ &\quad \left. - \frac{p^2 + M^2 - m^2}{2p^2} \log\left(\frac{M^2}{m^2}\right) \right. \\ &\quad \left. - \frac{1}{2} \sqrt{\Delta_2} \log\left[\frac{(1 + \sqrt{\Delta_2})p^2 - m^2 - M^2}{(1 - \sqrt{\Delta_2})p^2 - m^2 - M^2} \right] \right\}, \end{aligned} \quad (\text{B10})$$

where we have introduced the shorthand notation $\Delta_2 = (1 - \frac{m^2+M^2}{p^2})^2 - 4\frac{m^2M^2}{(p^2)^2}$. The above expression is valid for $0 < p^2 \leq (m - M)^2$; for $p^2 = (m - M)^2$, one has $\Delta_2 = 0$. In the kinematical region $(m - M)^2 < p^2 < (m + M)^2$, the two-point function is given by

$$B_0[p^2, m, M] = \frac{i}{(4\pi)^2} \left\{ \frac{2}{4-D} - \log\left(\frac{m^2}{\Lambda_B^2}\right) - \frac{p^2 + M^2 - m^2}{2p^2} \log\left(\frac{M^2}{m^2}\right) - \sqrt{-\Delta_2} \left[\arctan\left(\frac{p^2 + m^2 - M^2}{p^2 \sqrt{-\Delta_2}}\right) + \arctan\left(\frac{p^2 - m^2 + M^2}{p^2 \sqrt{-\Delta_2}}\right) \right] \right\}. \quad (\text{B11})$$

Finally, for $p^2 \geq (m + M)^2$, one has

$$B_0[p^2, m, M] = \frac{i}{(4\pi)^2} \left\{ \frac{2}{4-D} - \log\left(\frac{m^2}{\Lambda_B^2}\right) - \frac{p^2 + M^2 - m^2}{2p^2} \log\left(\frac{M^2}{m^2}\right) - \frac{1}{2} \sqrt{\Delta_2} \log\left[\frac{(1 + \sqrt{\Delta_2})p^2 - m^2 - M^2}{(1 - \sqrt{\Delta_2})p^2 - m^2 - M^2} \right] + i\pi\sqrt{\Delta_2} \right\}. \quad (\text{B12})$$

Tensor two-point integrals can be reduced to linear combinations of scalar one- and two-point functions. We consider here the case of a rank one tensor,

$$B^\mu[p^2, m, M] = \int \frac{d^D q}{(2\pi)^D} \frac{\mu^{(4-D)} q^\mu}{(q^2 - m^2 + i\epsilon)[(q-p)^2 - M^2 + i\epsilon]} = B_1[p^2, m, M] p^\mu, \quad (\text{B13})$$

where

$$B_1[p^2, m, M] = \frac{p^2 + m^2 - M^2}{2p^2} B_0[p^2, m, M] + \frac{A_0[M] - A_0[m]}{2p^2}. \quad (\text{B14})$$

-
- [1] T. Appelquist and J. Carazzone, *Phys. Rev. D* **11**, 2856 (1975).
[2] M. J. G. Veltman, *Nucl. Phys.* **B123**, 89 (1977).
[3] J. J. van der Bij and F. Hoogeveen, *Nucl. Phys.* **B283**, 477 (1987).
[4] R. Barbieri, M. Beccaria, P. Ciafaloni, G. Curci, and A. Vicere, *Phys. Lett. B* **288**, 95 (1992); **312**, 511(E) (1993); R. Barbieri, M. Beccaria, P. Ciafaloni, G. Curci, and A. Vicere, *Nucl. Phys.* **B409**, 105 (1993).
[5] J. Fleischer, O. V. Tarasov, and F. Jegerlehner, *Phys. Lett. B* **319**, 249 (1993).
[6] G. Degrassi, S. Fanchiotti, F. Feruglio, B. P. Gambino, and A. Vicini, *Phys. Lett. B* **350**, 75 (1995); G. Degrassi, P. Gambino, and A. Vicini, *Phys. Lett. B* **383**, 219 (1996).
[7] J. J. van der Bij, K. G. Chetyrkin, M. Faisst, G. Jikia, and T. Seidensticker, *Phys. Lett. B* **498**, 156 (2001).
[8] M. Faisst, J. H. Kuhn, T. Seidensticker, and O. Veretin, *Nucl. Phys.* **B665**, 649 (2003).
[9] D. Bettinelli and J. J. van der Bij, *Phys. Rev. D* **82**, 045020 (2010).
[10] D. Bettinelli and J. J. van der Bij, *Phys. Lett. B* **697**, 15 (2011).
[11] M. B. Einhorn, *Nucl. Phys.* **B246**, 75 (1984).
[12] K. Aoki, *Phys. Rev. D* **44**, 1547 (1991).
[13] M. Beneke, *Phys. Rep.* **317**, 1 (1999).
[14] K. Aoki and S. Peris, *Z. Phys. C* **61**, 303 (1994); *Phys. Rev. Lett.* **70**, 1743 (1993); K. Aoki, *Phys. Rev. D* **49**, R1167 (1994).
[15] T. Binoth and A. Ghinculov, *Phys. Rev. D* **56**, 3147 (1997); A. Ghinculov, T. Binoth, and J. J. van der Bij, *Phys. Rev. D* **57**, 1487 (1998); T. Binoth, A. Ghinculov, and J. J. van der Bij, *Phys. Lett. B* **417**, 343 (1998); T. Binoth and A. Ghinculov, *Nucl. Phys.* **B550**, 77 (1999); A. Ghinculov and T. Binoth, *Phys. Rev. D* **60**, 114003 (1999); R. Akhoury, J. J. van der Bij and H. Wang, *Eur. Phys. J. C* **20**, 497 (2001).
[16] G. Feldman, *Proc. R. Soc. A* **223**, 112 (1954); N. N. Bogoliubov and D. V. Shirkov, *Nuovo Cimento* **3**, 845 (1956).
[17] D. V. Shirkov and I. L. Solovtsov, *arXiv:hep-ph/9604363*; D. V. Shirkov and I. L. Solovtsov, *Phys. Rev. Lett.* **79**, 1209 (1997); I. L. Solovtsov and D. V. Shirkov, *Phys. Lett. B* **442**, 344 (1998); D. V. Shirkov, *Nucl. Phys. B, Proc. Suppl.* **64**, 106 (1998).
[18] R. Akhoury, J. J. van der Bij, and H. Wang, *Eur. Phys. J. C* **20**, 497 (2001).
[19] A. I. Alekseev, *Few-Body Syst.* **40**, 57 (2006); C. Ayala, C. Contreras, and G. Cvetič, *Phys. Rev. D* **85**, 114043 (2012).